Absorption of methane broadened by carbon dioxide in the 3.3 μm spectral region: From line centers to the far wings

H. Tran, J. Vander Auwera, T. Bertin, W. Fakhardji, O. Pirali, J. -M. Hartmann

Absorption of methane broadened by carbon dioxide in the 3.3 μm spectral region: from line centers to the far wings

H. Tran[1,#], J. Vander Auwera[2], T. Bertin[2], W. Fakhardji[1], O. Pirali[3,4], J.-M. Hartmann[1]

[1]*Laboratoire de Météorologie Dynamique/IPSL, CNRS, Ecole polytechnique, Institut Polytechnique de Paris, Sorbonne Université, Ecole Normale Supérieure, PSL Research University, F-91120 Palaiseau, France*

[2]*SQUARES, Université Libre de Bruxelles, C.P. 160/09, B-1050 Brussels, Belgium*

[3]*AILES beamline SOLEIL Synchrotron, L'Orme des Merisiers, 91190 Saint-Aubin, France*

[4] *Université Paris-Saclay, CNRS, Institut des Sciences Moléculaires d'Orsay, 91405 Orsay*

corresponding author: ha.tran@lmd.jussieu.fr

Abstract

This work studied the infrared absorption of methane broadened by carbon dioxide, which can contribute to the radiative budget of CO_2-dominated atmospheres. Fourier transform absorption spectra of CH_4 perturbed by CO_2 were recorded in the 3.3 μm spectral region, at room temperature and total pressures ranging from 3 to 25 bars. These experimental data were modeled using a theoretical approach taking collision-induced line mixing into account. Comparisons between measured and calculated spectra demonstrate that the proposed model is capable of accurately representing the absorption of methane broadened by collisions with CO_2, from line centers to the far wings. For practical applications, this rigorous spectral modeling was used to derive a simple χ-factor model to represent the spectral shape of CO_2-broadened CH_4 line wings. Comparisons with experimental values show that, at room temperature, the proposed χ-factor reproduces the measured spectra to within 10% in the band wings where the absorption is mainly due to the far line wings, while the usual Lorentzian profile leads to relative differences several orders of magnitude larger. This line-shape correction was successfully validated through comparisons with heavily saturated spectra of the ν_3 band of methane recorded at sub-atmospheric pressures.

1. Introduction

Molecular absorption in the far line wings is known to significantly contribute to the radiative budget of many planets (e.g. those of H_2O for the Earth atmosphere, of CO_2 for Venus and of CH_4 for Titan and Jupiter). This has motivated numerous experimental and theoretical laboratory studies of the far wing absorptions of various molecular systems [e.g. (Hartmann et al., 2018; Tran et al., 2018; Tran et al., 2019; Hartmann et al., 2021) and references therein]. To understand the climate of early Mars (Wordsworth 2016; Haberle et al., 2017; Ramirez and Kaltenegger, 2018) at the time when valley networks were carved by liquid water, it has been proposed that significant amounts of hydrogen and methane could have accumulated in the atmosphere 3-4 billion years ago (Ramirez et al., 2014; Chassefièere et al., 2016; Tarnas et al., 2018; Haberle et al., 2019; Kite et al., 2020). With this aim in view, several experimental and theoretical studies have been performed to determine the far-infrared absorptions induced

by collisions between CH_4 (and H_2) and CO_2. The first modeling of these collision-induced absorptions (CIAs) was based on those of CH_4-N_2 (and H_2-N_2) interacting pairs (Ramirez et al., 2014). In (Wordsworth et al., 2017), theoretical calculations of these CIAs were performed using a semi-empirical model that assumed that the shape of the CIA spectrum of CH_4-CO_2 (H_2-CO_2) can be calculated as a linear combination of the CO_2-CO_2 and CH_4-CH4 (H_2-H_2) CIAs (Richard et al., 2012). The CH_4-CO_2 (H_2-CO_2) CIA integrated intensity was then predicted based on ab initio calculations of the zeroth order spectral moment (Wordsworth et al., 2017). The results showed that the obtained CH_4-CO_2 and H_2-CO_2 CIAs are much more intense than those of CH_4-N_2 and H_2-N_2. The first measurements of these far-infrared CIAs were then performed in (Turbet et al., 2019) where it was shown that the calculated values of (Wordsworth et al., 2017) are overestimated by a factor of 1.6-1.7. In (Turbet et al., 2020), a new set of measurements of both CH_4-CO_2 and H_2-CO_2 CIAs was carried out, confirming the results of (Turbet et al., 2019), with reduced uncertainties. A semi-empirical model was also proposed in (Turbet et al., 2019), based on these measurements, which enabled to calculate CH_4-CO_2 and H_2-CO_2 CIAs over broad spectral (0-1500 cm^{-1}) and temperature (100-600 K) ranges.

The present work complements these studies through the measurement and modeling of absorption in the far wings of the lines of the CH_4 monomer broadened by CO_2 in the 3.3 μm spectral region, which can contribute to the greenhouse warming in CO_2-dominated atmospheres. Spectra of CH_4 highly diluted in CO_2 have been recorded, at room temperature and in a wide pressure range, using two different setups. The experimental setups and conditions are presented in Sec. 2. In Sec. 3, the spectral modeling, considering the effect of collisional line mixing, is described, and comparisons between measured and calculated spectra are presented. In Sec. 4, we propose an empirical χ-factor model to represent the spectral shape of CO_2-broadened CH_4 line wings. This model is determined from the most rigorous spectral modeling presented in Sec. 3 and validated using measured spectra. The conclusions of this work are drawn in Sec. 5.

2. Experiments

2.1 Measurements at ULB

Unapodized absorption spectra of CH_4+CO_2 mixtures and of pure CO_2 have been recorded using a Bruker IFS 120 upgraded to 125 HR Fourier transform spectrometer (FTS). For all the spectra, the instrument was fit with a globar source, a 0.8-mm entrance aperture diameter, a KBr beamsplitter, a band pass filter and an InSb detector cooled down to 77 K. Except when stated otherwise, the spectra were recorded at a resolution of 0.1 cm^{-1}, corresponding to a maximum optical path difference of 9 cm. A band-pass optical filter was used to only record the spectral range from 1800 to 5300 cm^{-1}, covering the entire ν_3 band of CH_4. Methane (99.998 % purity) and carbon dioxide (99.995 % purity) were purchased from Air Liquide. During the measurements, the gas mixtures were contained in a high-pressure cell providing an absorption path length of 10.16 m, optically coupled under vacuum to the FTS. The methane pressures were measured using MKS Baratron gauges model 690 of 10 Torr full scale range (Spectrum "No. 1" in Table 1) or model 626 of 1000 Torr full scale range (Spectra "No. 5" and "No. 9" in Table 1). The total pressures were measured using a MKS Baratron gauge model 627F of 25000 Torr full-scale range, directly connected to the high-pressure cell. The model 690 and 627F gauges were temperature stabilized at 45° Celsius. All the gauges

are characterized by an accuracy of reading conservatively assumed to be 0.5 %. The cell was wrapped in 5 cm thick stone wool and its temperature measured using 4 PT-111 platinum sensors (Lakeshore Cryotronics) characterized by an accuracy of reading better than 0.1 %, fixed at several locations on the outside wall.

Two series of spectra were recorded. In the first one, a mixture of CH_4 and CO_2 (mixture no. 1 in Table 1) at an initial total pressure (P_{tot}) of 24.53 atm and initial partial pressure of CH_4 (P_{CH4}) of 0.428 mbar was considered. The mixture was prepared in the cell, filling it with methane followed by carbon dioxide. A first spectrum (identified as "No. 1" in Table 1) was recorded under these sample conditions. The total pressure was then reduced to 12.36 atm and a second spectrum recorded at a resolution of 0.05 cm^{-1} ("No. 2" in Table 1). Using the same procedure, two other spectra were recorded at total pressures of 6.17 atm ("No. 3" in Table 1) and 3.08 atm ("No. 4" in Table 1) and higher resolution. The corresponding transmission spectra being not saturated, these spectra enable to study the effect of pressure on the absorption in the central region and near wings of the band. To achieve good accuracy on the absorption in a wide spectral range, i.e. from the center of the ν_3 band to its far wing, the second set of transmission spectra (identified as mixtures nos. 2 and 3 in Table 1) involved different CH_4 partial pressures for a fixed value of the total pressure. For mixture no. 2, the cell was first filled with 404 mbar of CH_4 and the total pressure brought to 24903 mbar with CO_2. A first spectrum ("No. 5" in Table 1) was recorded. The total pressure was then reduced by a factor F of about 10, CO_2 added to bring the total pressure to 25003.6 mbar (effectively dividing by F the partial pressure of methane) and spectrum "No. 6" was recorded. This procedure was repeated two more times, leading to spectra "No. 7" and "No. 8". The cell was evacuated, a new CH_4+CO_2 mixture (no. 3) prepared and spectra "No. 9" to "No. 13" were measured following the procedure applied to mixture no. 2. Pure CO_2 spectra $S_{CO2}(Ptot, \sigma)$ were also recorded at the same total pressures and resolutions as spectra No. 1 to 4 (Table 1).

The uncertainties on the methane pressures provided in Table 1 were estimated as follows. The uncertainties listed for spectra "No. 5" and "No. 9" are equal to 0.5% of P_{CH4}. The uncertainty on the low methane pressure measured for spectrum "No. 1" was conservatively set to 2.5% of P_{CH4} (Cacciani et al., 2022). The uncertainties on P_{CH4} for spectra of samples resulting from the dilution (i.e. spectra "No. 6" to "No. 8" and "No. 10" to "No. 13") were estimated by adding in quadrature the estimated uncertainty on P_{CH4} for the previous spectrum and the uncertainty ΔF on the factor F, estimated to be $\Delta F = \sqrt{2(0.5)^2} \approx 0.71\%$ of the reduced methane pressure.

The transmissions due to CH_4 broadened by CO_2 were obtained by dividing the signal obtained with the mixture, $S_{CH4+CO2}(Ptot, \sigma)$, by $S_{CO2}(Ptot, \sigma)$. With this procedure, the contribution of CO_2 absorption (the wings of neighboring CO_2 vibrational bands and some weak collision-induced absorption bands) could be removed. The absorption coefficients were then extracted from the transmissions thus obtained and normalized by the CH_4 partial pressure. Since most of the studied gas samples contain mixing ratios of methane smaller than 0.55%, the contribution of CH_4-CH_4 collisions is negligible. The contribution of CH_4-CH_4 collisions being not negligible for spectra No. 5 and 9, it was taken into account assuming that the effects of CH_4-CH_4 and of CH_4-CO_2 collisions are the same. This is justified by the fact that the average ratio of self- to air-broadening coefficients of CH_4 is 1.27 (Pine, 1992), very close to the ratio of CO_2 to air-broadenings (1.3, see Sec.3). As shown in Fig. 1 for mixture no. 2, the whole ν_3 band was then reconstructed by combining the spectral windows in which

the transmissions were between 0.2 and 0.8. The analysis of the second series of spectra recorded at ULB therefore resulted in two CH_4 partial-pressure-normalized absorption spectra of CH_4 broadened by CO_2 measured at average total pressures of 24991 mbar (mixture no. 2) and 24978 mbar (mixture no. 3) and an average temperature of 295.7 K.

Mixture	No.	$P_{tot}(\Delta P)$ / mbar	T (ΔT) / °C	$P_{CH4}(\Delta P)$ / mbar	Res. / cm^{-1}
1	1	24851 (17)	23.72 (0.12)	0.428 (11)	0.1
	2	12521.2 (2.9)	22.52 (0.01)	0.216 (6)	0.05
	3	6255.1 (2.0)	22.28 (0.08)	0.108 (3)	0.025
	4	3122.9 (1.3)	22.16 (0.02)	0.054 (1)	0.0125
2	5	24903 (12)	23.30 (0.08)	404 (2)	0.1
	6	25003.6 (6.0)	22.68 (0.04)	42.1 (4)	0.1
	7	25029.4 (6.0)	22.68 (0.04)	4.20 (5)	0.1
	8	25029 (13)	22.70 (0.08)	0.428 (6)	0.1
3	9	24764 (14)	22.85 (0.11)	1241 (6)	0.1
	10	24990.2 (8.0)	22.71 (0.06)	130.3 (1.1)	0.1
	11	25025.2 (3.3)	22.62 (0.03)	13.16 (15)	0.1
	12	25052.0 (2.0)	22.62 (0.01)	1.345 (18)	0.1
	13	25074.8 (8.1)	22.63 (0.07)	0.1376 (21)	0.1

Table 1: Experimental conditions for the CH_4+CO_2 spectra measured with the ULB setup. Spectra of pure CO_2 were recorded for the same pressure conditions as spectra No. 1 to 4. The numbers between parentheses provided for the pressures and temperatures are the estimated uncertainties. For the total pressure P_{tot} and the temperature T, they are the variations of these quantities during the recordings, the estimated accuracy of measurement of the pressure (0.5% of reading) and of the temperature (0.1% of reading) being not included. The estimation of the uncertainties on the methane pressures is detailed in the text.

Note that the measured and reconstructed spectra were corrected to get rid of possible errors in the partial pressures of methane. This was done by multiplying the experimental results by a constant factor such that the integrated absorptions of the measured spectrum and of the corresponding calculated one match. The correction factors vary from 0.96 to 1.1 depending on the spectrum. They are larger than the estimated uncertainties on the methane pressures and probably a better assessment of these. No correlation was found between the correction factors and the CH_4 pressures.

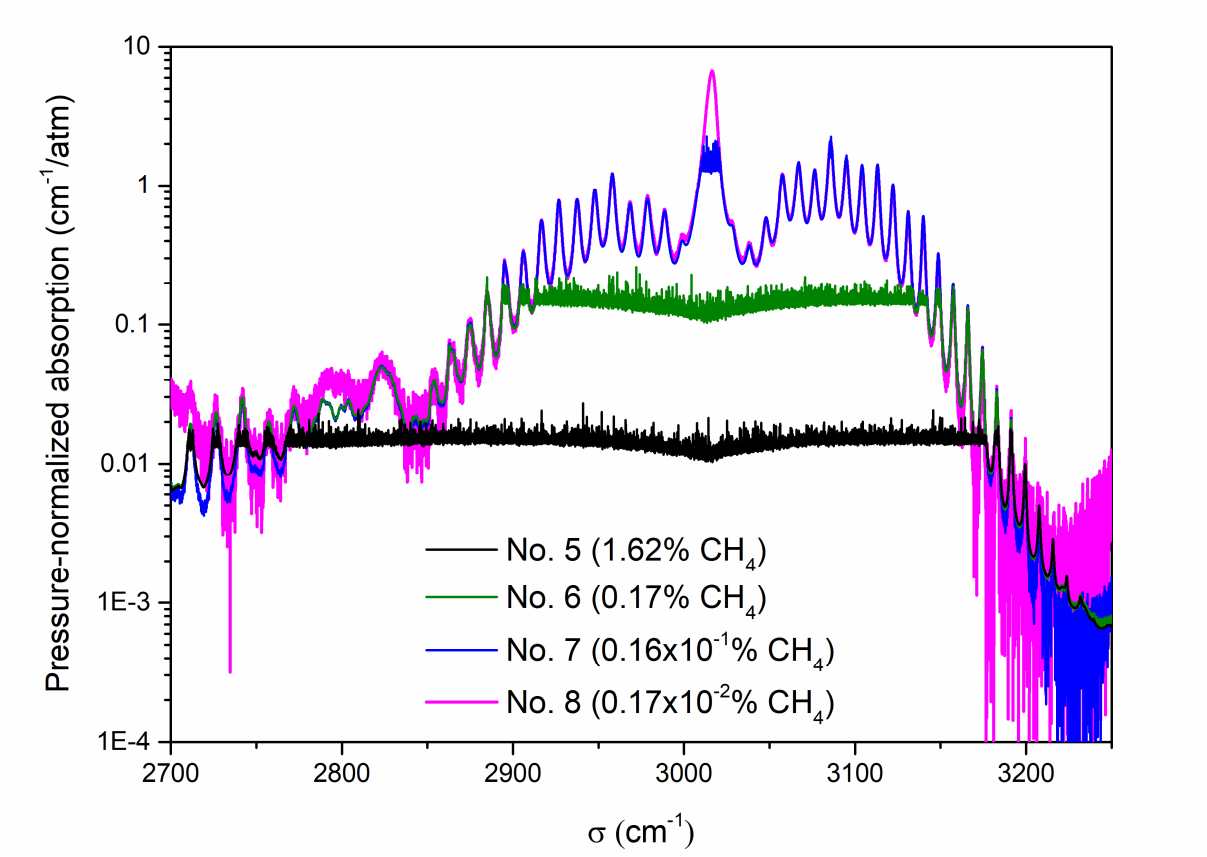

Figure 1: CH_4 partial-pressure-normalized absorption spectra of CH_4 broadened by CO_2 measured at an average total pressure of 24991 mbar and for various partial pressures of CH_4 (mixture no. 2 in Table 1).

2.2. Measurements at SOLEIL

CH_4+CO_2 transmittance spectra were also measured using the facilities at the AILES beam line of the SOLEIL synchrotron. The experimental setup is composed of a Fourier transform spectrometer Bruker IFS 125 HR equipped with a globar source and a KBr beamsplitter from which the incident light beam goes into a 2.5 m long multi-pass cell closed with diamond windows, set for an optical path of 101.3 m. The transmitted light was received by a HgCdTe detector cooled down with liquid nitrogen. Each spectrum has a usable part between 800 and 4600 cm^{-1} and results from the average of 1000 interferograms recorded with an unapodized resolution of 0.5 cm^{-1}.

The experiments proceeded as follows. The cell was filled with 54.4 mbar of CH_4 and CO_2 was added until a total pressure of 945.7 mbar was reached (the pressures were measured with a 0 - 1000 mbar Pfeiffer gauge), resulting in a methane mole fraction of about 5 %. The mixture was let to evolve freely for 10 to 15 minutes to reach equilibrium and the absorption spectrum of the mixture was recorded. The total pressure was then reduced to 764.2 mbar, the mixture given 10 to 15 minutes to reach equilibrium and the spectrum of the mixture recorded. The procedure was then repeated for total pressures of 607.3, 480.0, 378.3, 171.6, 107.1 and 58.3 mbar. A reference spectrum was also recorded with the cell filled with about 1 bar of pure argon to generate transmittance spectra for all the total pressures.

3. Spectral modeling: line-mixing effect

It is well known that collisional interferences (line-mixing) play an important role in the infrared absorption spectrum of methane [see (Pieroni et al., 1999; Tran et al., 2006a) for instance]. Within the impact approximation and including line-mixing effects, the infrared absorption coefficient α (cm^{-1}) at wavenumber σ (cm^{-1}) of CH_4 broadened by CO_2 is given by (Hartmann et al., 2021):

$$\alpha^{LM}(\sigma, P_{CH4}, P_{CO2}, T) = \frac{8\pi^2\sigma}{3hc}\left[1 - \exp\left(-\frac{hc\sigma}{k_B T}\right)\right] \times \frac{P_{CH4}}{k_B T}$$

$$\times Im\{\sum_\ell \sum_k \rho_\ell(T) d_\ell d_k \langle\langle k \| [\boldsymbol{\Sigma} - \boldsymbol{L_0} - iP_{CO2}\boldsymbol{W}(T)]^{-1} \| \ell \rangle\rangle\} \,. \quad (1)$$

In Eq. (1), the sums extend over all the absorption lines ℓ and k of CH_4; P_{CH4} and P_{CO2} are the partial pressures of CH_4 and CO_2, respectively; T is the temperature (in kelvin); h, c and k_B are the Planck constant, the speed of light in vacuum and the Boltzmann constant. ρ_ℓ and d_ℓ are the relative population of the initial level and the dipole matrix element of line ℓ. $\boldsymbol{\Sigma}$, $\boldsymbol{L_0}$ and $\boldsymbol{W}$ are operators in the Liouville space and $\langle\langle k \| \ldots \| \ell \rangle\rangle$ designates a matrix element. The first two are diagonal, associated with the current wavenumber and the positions of the lines. $\boldsymbol{W}$ is the relaxation matrix which describes the effect of collisions between CH_4 and CO_2 on the CH_4 optical transitions. In this equation, we neglected the self-broadening effect as explained in Sec. 2.1, the Doppler term and the influence of velocity changes as well as the speed dependences of the relaxation matrix $\boldsymbol{W}$. The latter contains the influence of collisions on the spectral shape. It depends on the band, on the temperature and on the collisional partner. Its off-diagonal elements lead to collisional interferences between lines while the real and imaginary diagonal terms are the pressure-broadening, γ_ℓ, and -shifting, δ_ℓ, of the isolated lines, i.e.

$$\langle\langle \ell \| \boldsymbol{W}(T) \| \ell \rangle\rangle = \gamma_\ell(T) - i\delta_\ell(T) \,. \quad (2)$$

When line mixing is disregarded, $\boldsymbol{W}$ is diagonal and Eq. (1) becomes the usual sum of Lorentzian contributions.

The off-diagonal imaginary elements of $\boldsymbol{W}$ are neglected while the real elements are computed, as done in (Pieroni et al., 1999; Tran et al., 2006), using:

$$\langle\langle k \| \boldsymbol{W}(T) \| \ell \rangle\rangle = -A_{k,\ell} \times K(i_k \leftarrow i_\ell, T), \quad (3)$$

where $K(i_k \leftarrow i_\ell, T)$ denotes the state-to-state collisional transfer rates from the initial level of line ℓ to the initial level of line k; the parameters $A_{k,\ell}$ enable switching from the state space to the line space, as explained in (Pieroni et al., 1999).

Spectra were calculated for the pressure and temperature conditions of the experiments. Since the considered region is dominated by the ν_3 band of $^{12}CH_4$, calculations with line-mixing taken into account were performed only for the lines of this band. The other lines (minor isotopologues, hot bands) were calculated with the Voigt profile. The individual line parameters, i.e. the unperturbed line position, integrated intensity, energy of the lower state, were taken from the 2020 edition of the HITRAN database (Gordon et al., 2022). The populations and the dipole matrix elements were deduced from these data [as done in (Tran et al., 2006a)]. The pressure-broadening coefficients of CH_4 lines by CO_2 were obtained by multiplying by 1.3 the air-broadening coefficients provided by the package of (Tran et al., 2006a). This factor, which is close to the value of 1.21 obtained by averaging the ratio

between the CO_2-broadening coefficients of 28 CH_4 lines measured by (Fissiaux et al., 2014) and the corresponding values for air-broadening [taken from (Tran et al., 2006a) and references therein], was retained because it gives the best agreement between the spectra calculated and measured in the present work. In the absence of available measured or calculated data, we assumed that the pressure-shifting coefficients of CH_4 by collisions with CO_2 are the same as those of CH_4 by air. The latter were also provided by the package of (Tran et al., 2006a). Note that the air-broadening and -shifting coefficients in (Tran et al., 2006a) were obtained from the measured data of (Pine, 1997) in which these parameters were determined with line-mixing effect taken into account. These data are thus consistent with the line-shape model used here.

The off-diagonal elements of the relaxation matrix, including the state-to-state rates $K(i_k \leftarrow i_\ell, T)$ and the $A_{k,\ell}$ parameters, were assumed to be proportional to those for CH_4 in N_2, also provided in (Tran et al., 2006a), with the same multiplicative factor as for the line broadening coefficients, i.e. $\langle\langle k \left\| \boldsymbol{W^{CH4/CO2}}(T) \right\| \ell \rangle\rangle = 1.3 \times \langle\langle k \left\| \boldsymbol{W^{CH4/N2}}(T) \right\| \ell \rangle\rangle$. Detailed information on the state-to-state rates $K(i_k \leftarrow i_\ell, T)$ and the $A_{k,\ell}$ parameters can be found in (Tran et al., 2006a) and references therein.

Figures 2 and 3 show examples of comparison between measured spectra (mixture no. 1 in Table 1) and those calculated as described above for the same pressure and temperature conditions. In addition to the predictions made taking line-mixing into account, the spectra calculated with the same spectroscopic parameters but using the Voigt profile (i.e. neglecting line-mixing effect) are also displayed. The density of CO_2 was determined from the measured pressure and temperature using NIST-recommended equation of state taking into account the fact that the gas is not ideal.[i] As can be observed, the line-mixing calculations, although not perfect, lead to much better agreements with the measurements, the root mean square of the obtained residuals being more than twice smaller than that for the Voigt calculations. These results are consistent with those obtained previously for CH_4 broadened by N_2 (Pieroni et al., 1999; Tran et al., 2006a) in which a detailed analysis of the influence of line-mixing effects on the absorption spectrum can be found.

[i] https://webbook.nist.gov/cgi/cbook.cgi?Source=1927LOW%2FERI2729-2734&Units=SI&Mask=7

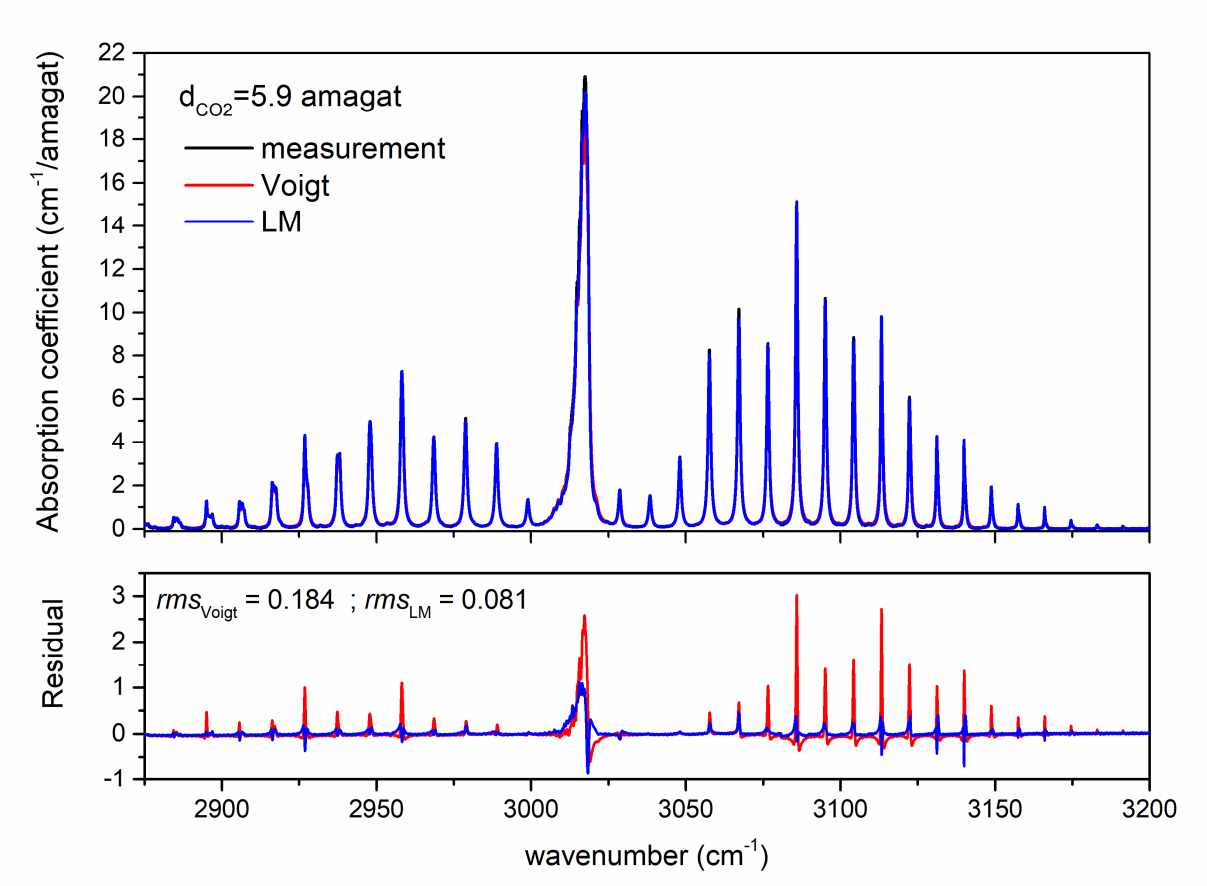

Figure 2: Comparison between the CO_2-broadened CH_4 spectrum measured (black) at room temperature for a density of CO_2, (d_{CO2}) of 5.9 amagat (spectrum No. 3 in Table 1; 1 amagat corresponding to 2.687 10^{19} molec.cm^{-3} at 273.15 K) and values calculated with (blue) and without (red) line mixing taken into account.

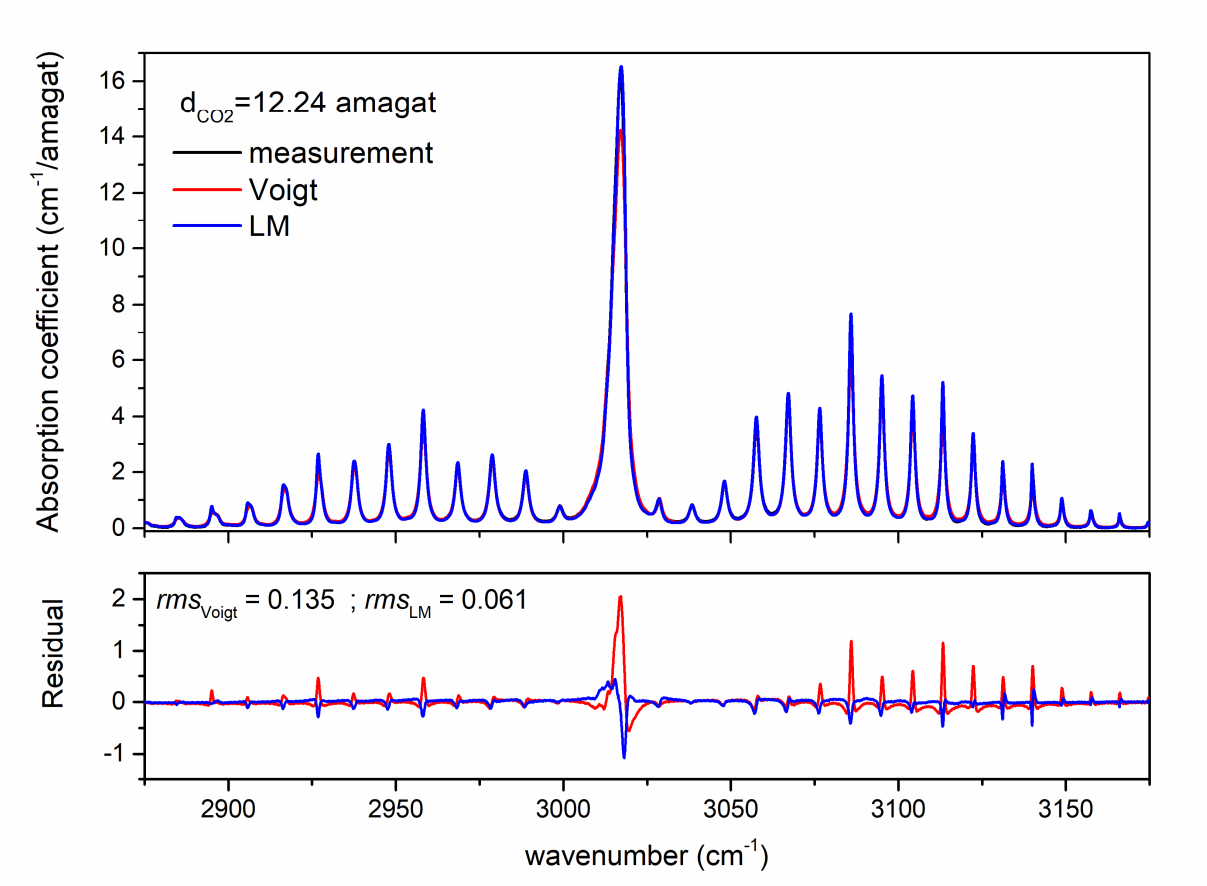

Figure 3: Same as Fig. 2 for d_{CO2}=12.24 amagat (spectrum no. 2 in Table 1).

The absorption in the band wing is displayed in Fig. 4 where calculations with and without line-mixing are compared with the spectra reconstructed (see Sec. 2.1) from measurements for the mixtures nos. 2 and 3 of Table 1. Again, the calculation with line-mixing leads to a good agreement with the measurements, especially in the blue wing of the band. Absorption in this spectral region is mainly due to the cumulating far wings of the strong ν_3 lines close to the center of the band. For CH_4, it is well known that the Voigt profile strongly overestimates absorption in the far line wings (Hartmann et al., 2002; Tran et al., 2006a; Tran et al., 2006b), which is also observed here. Furthermore, in the troughs between the manifolds, particularly in the R branch, taking line-mixing into account also significantly improves the agreement with the measurements, when compared with the purely Voigt calculation. This result shows that our model, although quite simple since based on an approach developed for N_2-broadened CH_4 lines, is capable to accurately predict the absorption shape from resonances to the far wings of CH_4 perturbed by CO_2.

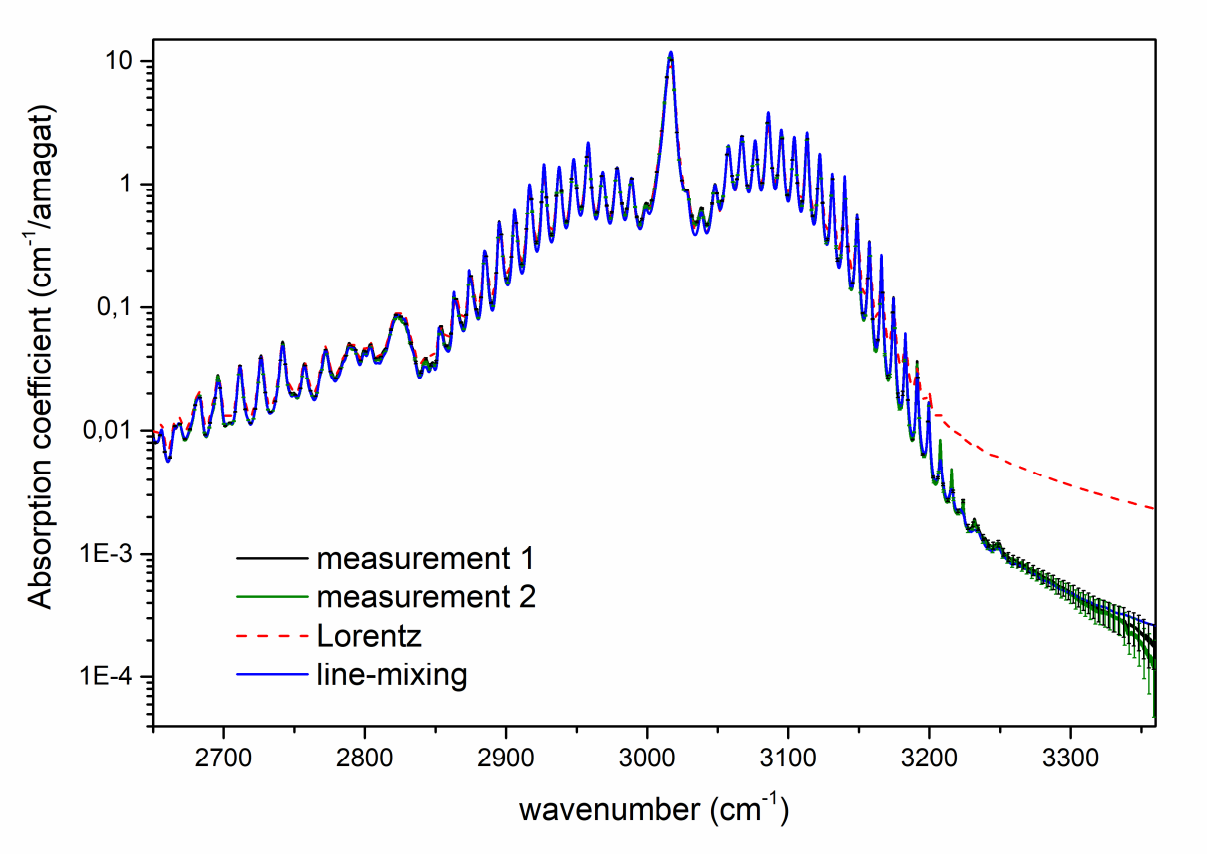

Figure 4: Comparison between CO_2-broadened CH_4 spectra measured at d_{tot} = 26.5 amagat (in olive and black, corresponding to mixtures no. 2 and 3 of Table 1) and values calculated with (blue) and without (red) line-mixing taken into account. The error bars on the measured absorption coefficient represent the uncertainties due to those of the baselines and the subtracted CO_2 absorption contributions (estimated to be 1%).

4. χ-factor model for the far wings of CO_2-broadened CH_4 lines

For practical applications such as simulations of planetary atmospheres spectra, Lorentzian (or Voigt) line shapes with line wings corrected using a χ-factor are widely used. Within this simple model, the absorption coefficient of a highly diluted CH_4-CO_2 mixture is written as:

$$\alpha(\sigma, P_{CH4}, P_{CO2}, T) = \frac{1}{\pi}\sum_{\ell} P_{CH4} S_\ell(T) \times exp\left[\frac{hc(\sigma-\sigma_\ell)}{2k_BT}\right]\frac{\sigma}{\sigma_\ell}\frac{1-e^{-\frac{hc\sigma}{k_BT}}}{1-e^{-\frac{hc\sigma_\ell}{k_BT}}}\frac{P_{CO2}\gamma_\ell(T)}{(\sigma-\sigma_\ell)^2+\left(P_{CO2}\gamma_\ell(T)\right)^2}\chi(|\sigma-\sigma_\ell|,T) \quad (4)$$

The corrective factor χ, which is assumed to be the same for all lines, depends on the frequency detuning with respect to the line center and on the temperature. It is generally (Perrin and Hartmann, 1989; Hartmann et al., 2002; Tran et al., 2011) represented by analytical expressions with parameters deduced from fits of measured spectra. In this work, χ was determined by fitting Eq. (4) to absorption spectra in the region of the ν_3 band, calculated using the model described in Sec. 3 (taking line-mixing effect into account) for various pressure and temperature conditions. Note that the model described in Sec. 3 is based on a

theoretical approach developed for CH_4 perturbed N_2 (Pieroni et al., 1999; Tran et al., 2006a), which showed that it is capable to accurately represent absorption spectra of CH_4 in N_2 for large range of temperature (i.e. from 200 to 300 K). Here, we assume that the broadening coefficients and the off-diagonal elements of the relaxation matrix of CH_4 in CO_2 have the same temperature dependences as those of CH_4 in N_2. Therefore, the model of Sec. 3 can be used to simulate spectra at various temperatures. The following values for χ were obtained:

$$|\sigma - \sigma_\ell| = \Delta\sigma < \sigma_1 = 15 \text{ cm}^{-1}, \chi = 1$$

$$\sigma_1 < \Delta\sigma < \sigma_2 = 60 \text{ cm}^{-1}, \chi = \exp[-0.0375(\Delta\sigma - \sigma_1)] \quad (5)$$

$$\sigma_2 < \Delta\sigma \text{ , } \chi = \exp[-0.0375(\sigma_2 - \sigma_1) - \beta(T)(\Delta\sigma - \sigma_2)]$$

$$\text{with } \beta(T) = -5.3 \times 10^{-4} + 0.0194e^{-0.0041T}$$

Figure 5 shows comparisons between the absorption coefficients calculated using Eqs. (4,5) and those obtained with the model described in Sec. 3 for three different pressure and temperature conditions. Very good agreements in the blue wing of the band can be observed. Note that the χ-factor as proposed in Eqs. (4,5) allows for the correction of sub-Lorentzian effect in the line wings while it is equivalent to a Lorentzian (or Voigt) line shape in the line centers and near wings. In the band wings, where absorption is mainly due to the far line wings, the χ-factor approach leads to good agreements with measured spectra. For instance, at 3400 cm^{-1} and for d_{tot} = 26.5 amagat, the relative difference between the absorption coefficients computed with the χ-factor model and the measured spectra is about 10% while the usual Lorentzian profile leads to a relative difference of several order of magnitude. However, in regions of line centers and near wings, an accurate modeling of the measured absorptions requires taking into account properly line-mixing effect through the use of the full relaxation matrix as described in Sec. 3. The χ-factor model therefore should be used to model absorption in the far line wings only.

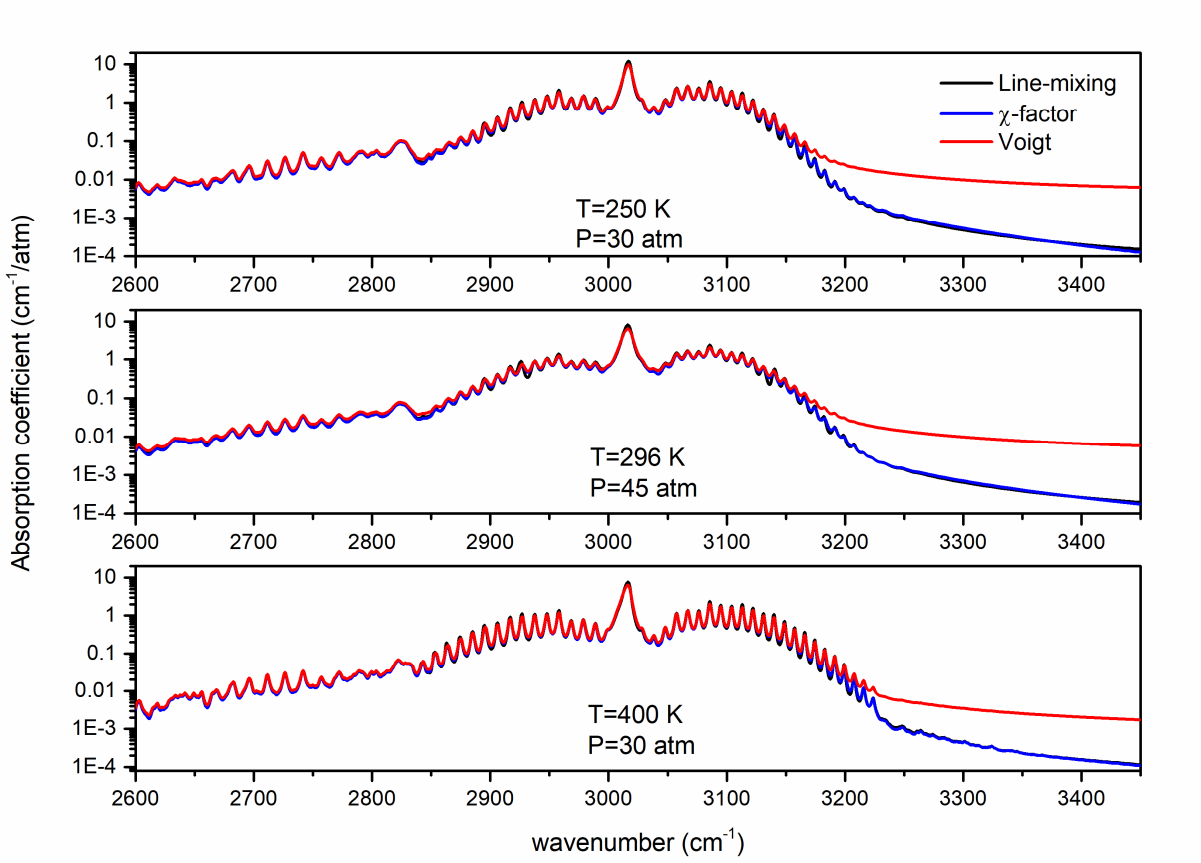

Figure 5: Absorption coefficients of CH_4 highly diluted in CO_2 calculated with (black line) and without (red) line mixing, at 250 K and 30 atm (top panel), 296 K and 45 atm (middle panel) and 400 K and 30 atm (bottom panel). Values calculated with the χ-factor model [see Eqs. (4,5)] are plotted in blue.

In (Gharavi and Buckley, 2005) devoted to the R(3) and R(4) manifolds of the $2\nu_3$ band, it was shown that the temperature dependences of CO_2- and N_2-broadening coefficients of CH_4 lines can be quite different. The ratio γ_{CO2}/γ_{N2} can indeed vary from 1.36 to 1.24 in the 296-670 K range. It is well known that the absorption coefficient in the line wing is proportional to the corresponding line width. Therefore, changing γ_{CO2}/γ_{N2} from 1.3 to 1.2 or to 1.4 leads to a difference of about 10% for the absorption coefficient in the wings. This is negligible compared to the difference between the absorption coefficient calculated with the Voigt line shape and that computed with the full line-mixing modeling (about one order of magnitude at 3300 cm^{-1}, for instance, see Figs. 4, 5). In the absence of accurate data for CO_2-broadening coefficients and their temperature dependences, the χ-factor proposed in this work can be therefore used in the 200 K-400 K temperature range.

The obtained χ-factor model was then used to compute spectra for the same conditions as those of the experiments recorded at SOLEIL (see Sec. 2.2). For the comparison with the measured spectra, absorption contributions due to CO_2 and to a small amount of water vapor (a H_2O fraction of $x_{H2O} = 9.5 \times 10^{-5}$ was retrieved from the measured spectra) were included in the calculation. Voigt profiles were used, and the needed spectroscopic data of CO_2 and H_2O were taken from (Gordon et al., 2022). Note that calculations using a χ-factor model for CO_2 line wings (Tran et al., 2011) were also performed to compute CO_2 absorption

contributions, showing that CO_2 line wings have negligible influence on the total absorptions. The CH_4-broadening coefficients of CO_2 lines were assumed to be the same as the air-broadenings. This approximation should not affect the results since the mole fraction of CH_4 is quite small ($x_{CH4} = 0.0575$). Figure 6 shows comparisons between the measured spectra and those computed using the χ-factor model proposed in this work as well as using purely Voigt line shapes, for the ν_3 band region. As can be observed, the spectra are largely saturated around the band center. In the red wing of the band, the two calculations are both in good agreement with the measurements. This can be explained by the large contribution of local lines in this region. In the blue wing of the band where the relative contribution of the far wings is more important, the χ-factor model accurately reproduces the measurements, contrary to the Voigt profile that largely overestimates absorptions. These results thus validate the χ-factor model [Eqs.(4) and (5)] at room temperature, which can now be used for applications as those mentioned in Sec. 1. Note that the remaining residuals, namely those observed around 3200 cm^{-1}, are probably due to the uncertainties of the spectroscopic data of the local lines (Gordon et al., 2022) but also to the use of a unique scaling factor to deduce CO_2-broadenings coefficients of methane lines from air-broadening coefficients.

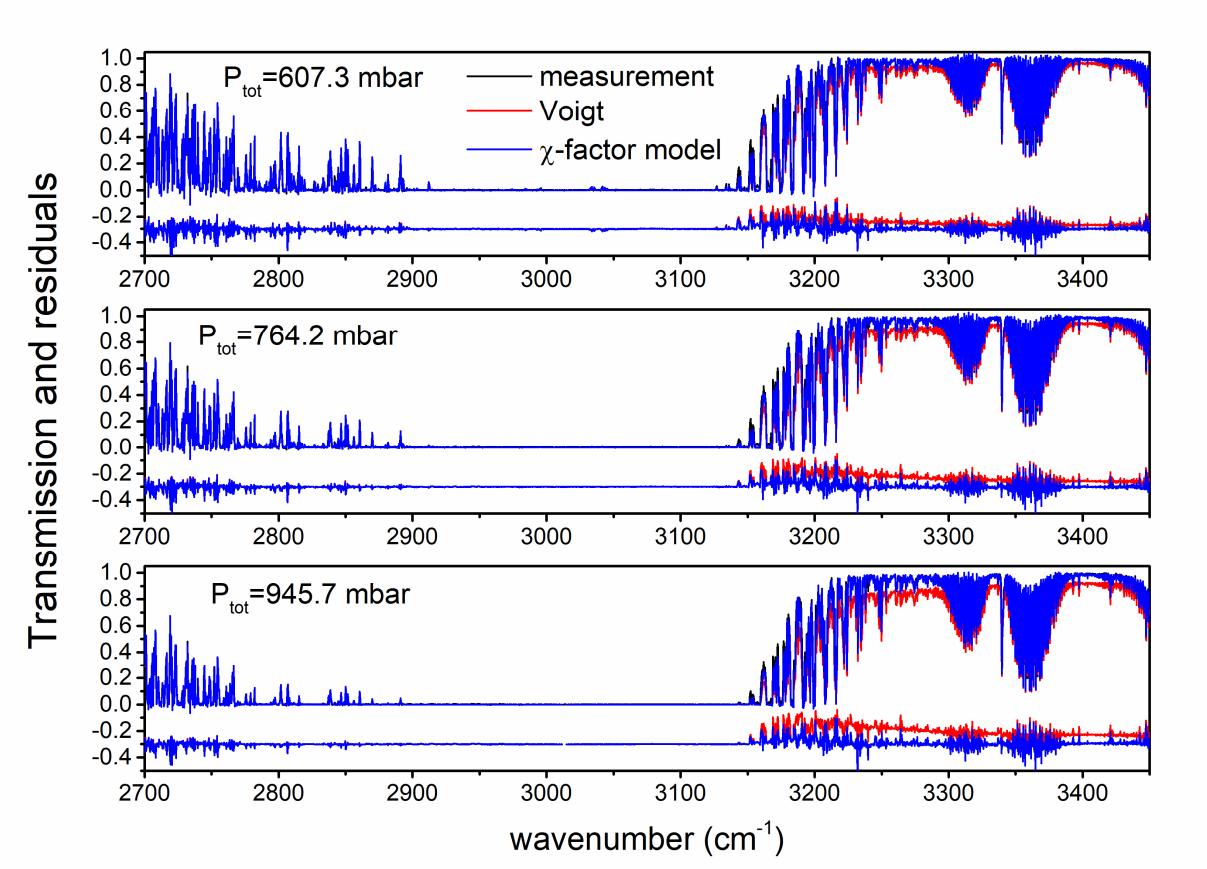

Figure 6: Comparison between the SOLEIL spectra measured (black) in the ν_3 band region at room temperature and various total pressures of a mixture of CH_4 in CO_2 with $x_{CH4} = 0.0575$ and calculations at the same conditions, using the χ-factor model (blue) and the usual Voigt line shape (red). The differences between the measured spectra and calculated values are also displayed in each corresponding panel (minus 0.3).

5. Conclusion

This article presented the first modeling of the spectral shape of methane absorption lines broadened by CO_2 from the line centers to the far wings. The model, based on a theoretical approach previously developed for N_2-broadened CO_2 absorption lines, accounted for the collision-induced line-mixing effects. Comparison with spectra measured in the CH_4 ν_3 band region at room temperature and for a broad pressure range showed that the model is capable to accurately reproduce absorption spectra of CH_4 in CO_2, from the line centers to the far wings, in contrast with the Voigt profile that leads to large discrepancies with the measurements. The model was then used to compute spectra of CH_4 in CO_2 for various pressure and temperature conditions (from 200 to 400 K), which enabled the determination of a simple line-shape correction factor χ in order to correct for the sub-Lorentzian behavior in the far line wings. The latter, successfully validated by comparison with experimental spectra, can be straightforwardly used to model absorption in the line wings, for practical applications such as radiative transfer calculations for a planetary atmosphere. Finally, it is worthy to note that the model can be largely improved in the future when accurate CO_2-broadening coefficients of CH_4 lines, their temperature dependences as well as the state-to-state collisional transfer rates are available.

Acknowledgements

This work was performed in the frame of the *Agence Nationale de la Recherche* (ANR) project COMPLEAT (ANR-19-CE31-0010-01). T. Bertin thanks the FRIA (*Fonds pour la Formation à la Recherche dans l'Industrie et l'Agriculture*, Belgium) for a PhD fellowship and J. Vander Auwera acknowledges financial support from the *Fonds de la Recherche Scientifique* – FNRS (Belgium, contract no. J.0217.20).

References

Cacciani, P, Cermák, P, Vander Auwera, J, Campargue, A, 2022. The ammonia absorption spectrum between 3900 and 4700 cm^{-1}. J. Quant. Spectrosc. Radiat. Transf. 277, 107961.

Chassefièere, E, Lasue, J, Langlais, B, Quesnel, Y, 2016. Early Mars serpentinization-derived CH_4 reservoirs, H_2-induced warming and paleo-pressure evolution. Meteorit. Planet. Sci. 51, 2234-45.

Fissiaux, L, Delière, Q, Blanquet, G, Robert, S, Vandaele, AC, Lepère, M, 2014. CO_2-broadening coefficients in the ν_4 fundamental band of methane at room temperature and application to CO_2-rich planetary atmospheres. J. Mol. Spectrosc. 297, 35-40.

Gharavi, M, Buckley, SG, 2005. Diode laser absorption spectroscopy measurement of linestrenghts and pressure broadening coefficients of the methane $2\nu_3$ band at elevated temperatures. J. Mol. Spectrosc. 229, 78-88.

Gordon, IE, Rothman, LS, Hargreaves, RJ, R Hashemi, EV Karlovets, FM Skinner, K Conway, C Hill, RV Kochanov, Y Tan, P Wcisło et al, 2022. The HITRAN2020 molecular spectroscopic database. J. Quant. Spectrosc. Radiat. Transf. 277, 107949. https://doi.org/10.1016/j.jqsrt.2021.107949

Haberle, R, Catling, D, Carr, M, Zahnle, K, 2017. The early Mars climate system. In: Haberle R, Clancy R, Forget F, Smith M, Zurek R (Eds.). The Atmosphere and Climate of Mars. Cambridge University Press, Cambridge, 526–568 Cambridge Planetary Science.

Haberle, RM, Zahnle, K, Barlow, NG, Steakley, KE, 2019. Impact degassing of H_2 on early Mars and its effect on the climate system. Geophys. Res. Lett. 46, 13355-62.

Hartmann, JM, Boulet, C, Brodbeck, C, Nguyen, VT, Fouchet, T, Drossart, P, 2002. A far wing lineshape for H_2 broadened CH_4 infrared transitions. J. Quant. Spectrosc. Radiat. Transf. 72, 117-122.

Hartmann, JM, Tran, H, Armante, R, Boulet, C, Campargue, A, Forget, F, et al, 2018. Recent advances in collisional effects on spectra of molecular gases and their practical consequences. J. Quant. Spectrosc. Radiat. Transf. 213, 178-227.

Hartmann, JM, Boulet, C, Robert, D, 2021. Collisional effects on molecular spectra: laboratory experiments and models, consequences for applications (2nd edition). Elsevier, Amsterdam.

Kite, ES, Mischna, M, Gao, P, Yung, YL, Turbet, M, 2020. Methane release on early Mars by atmospheric collapse and atmospheric reinflation. Planetary and Space Science 181, 104820.

Perrin, MY, Hartmann, JM, 1989. Temperature-dependent measurements and modeling of absorption by CO_2-N_2 mixtures in the far line wings of the 4.3 μm CO_2 band. J. Quant. Spectrosc. Radiat. Transf. 42, 311-317.

Pieroni, D, Nguyen, VT, Brodbeck, C, Claveau, C, Valentin, A, Hartmann, JM, Gabard, T, Champion, JP, Bermejo D, Domenech, JL, 1999. Experimental and theoretical study of line mixing in methane spectra. I. The N_2-broadened ν_3 band at room temperature. J. Chem. Phys. 110, 7717.

Pine, AS, 1992. Self-, N_2, O_2, H_2, Ar, and He broadening in the ν_3 band Q branch of CH_4. J. Chem. Phys. 97, 773.

Pine, AS, 1997. N_2 and Ar broadening and line mixing in the P and R branches of the ν_3 band of CH_4. J. Quant. Spectrosc. Radiat. Transf. 57, 157-76.

Ramirez, RM, Kopparapu, R, Zugger, ME, Robinson, TD, Freedman, R, Kasting, JF, 2014. Warming early Mars with CO_2 and H_2. Nat. Geosci. 7, 59–63.

Ramirez, RM, Kaltenegger, L, 2018. A methane extension to the classical habitable zone. Astrophys. J. 858, 72.

Richard, C, Gordon, IE, Rothman, LS, Abel, M, Frommhold, L, Gustafsson, M, Hartmann, JM, Hermans, C, Lafferty, WJ, Orton, GS, Smith, KM, Tran, H, 2012. New section of the HITRAN database: collision-induced absorption (CIA). J. Quant. Spectrosc. Radiat. Transf. 113, 1276-85.

Tarnas, JD, Mustard, JF, Sherwood, LB, Bramble, MS, Cannon, KM, Palumbo, AM, Plesa, AC, 2018. Radiolytic H_2 production on Noachian Mars: implications for habitability and atmospheric warming. Earth Planet Sci. Lett. 502, 133-45.

Tran, H, Flaud, JM, Gabard, T, Hase, F, von Clarmann, T, Camy-Peyret, C, Payan, S, Hartmann, JM, 2006a. Model, software and database for line-mixing effects in the ν_3 and ν_4 bands of CH_4 and tests using laboratory and planetary measurements. I: N_2 (and air) broadenings and the earth atmosphere. J. Quant. Spectrosc. Radiat. Transf. 101, 284-305. https://doi.org/10.1016/j.jqsrt.2005.11.020

Tran, H, Flaud, PM, Fouchet, T, Garbard, T, Hartmann, JM, 2006b. Model, software and database for line-mixing effects in the ν_3 and ν_4 bands of CH_4 and tests using laboratory and planetary measurements – II: H_2 (and He) broadening and the atmosphere of Jupiter and Saturn. J. Quant. Spectrosc. Radiat. Transf. 101, 306-324.

Tran, H, Boulet, C, Stefani, S, Snels, M, Piccioni, G, 2011. Measurements and modelling of high-pressure pure CO_2 spectra from 750 to 8500 cm^{-1}. I-central and wing regions of the allowed vibrational bands. J. Quant. Spectrosc. Radiat. Transf. 112, 925-936.

Tran, H, Turbet, M, Chelin, P, Landsheere, X, 2018. Measurements and modeling of absorption by CO_2+H_2O mixtures in the spectral region beyond the CO_2 ν_3-band head. Icarus 306, 116-21. https://doi.org/10.1016/j.icarus.2018.02.009

Tran, H, Turbet, M, Hanoufa, S, Landsheere, X, Chelin, P, Ma, Q, Hartmann, JM, 2019. The CO_2-broadened H_2O continuum in the 100-1500 cm^{-1} region: Measurements, predictions and empirical model. J. Quant. Spectrosc. Radiat. Transf. 230, 75-80. https://doi.org/10.1016/j.jqsrt.2019.03.016

Turbet, M, Tran, H, Pirali, O, Forget, F, Boulet, C, Hartmann, JM, 2019. Far infrared measurements of absorptions by CH_4+CO_2 and H_2+CO_2 mixtures and implications for greenhouse warming on early Mars. Icarus. 321, 189-99.

Turbet, M, Boulet, C, Karman, T, 2020. Measurements and semi-empirical calculations of CO_2+CH_4 and CO_2+H_2 collision-induced absorption across a wide range of wavelengths and temperature. Application for the prediction of early Mars surface temperature. Icarus. 346, 113762.

Wordsworth, RD, 2016. The Climate of Early Mars. Ann. Rev. Earth. Planet Sci. 44, 381-408.

Wordsworth, R, Kalugina, Y, Lokshtanov, S, Vigasin, A, Ehlmann, B, Head, J, Sanders, C, Wang, H, 2017. Transient reducing greenhouse warming on early Mars. Geophys. Res. Lett. 44, 665-71.